


Global transcriptome analysis of rat dorsal root ganglia to identify molecular pathways involved in incisional pain

Molecular Pain
Volume 16: 1–15
© The Author(s) 2020
Article reuse guidelines:
sagepub.com/journals-permissions
DOI: 10.1177/1744806920956480
journals.sagepub.com/home/mpx


Phu V Tran^{1,*}, Malcolm E Johns^{2,*}, Brian McAdams³,
Juan E Abrahante⁴, Donald A Simone³, and Ratan K Banik² 

Abstract

To develop non-opioid therapies for postoperative incisional pain, we must understand its underlying molecular mechanisms. In this study, we assessed global gene expression changes in dorsal root ganglia neurons in a model of incisional pain to identify pertinent molecular pathways. Male, Sprague–Dawley rats underwent infiltration of 1% capsaicin or vehicle into the plantar hind paw (n = 6–9/group) 30 min before plantar incision. Twenty-four hours after incision or sham (control) surgery, lumbar L4–L6 dorsal root ganglia were collected from rats pretreated with vehicle or capsaicin. RNA was isolated and sequenced by next generation sequencing. The genes were then annotated to functional networks using a knowledge-based database, Ingenuity Pathway Analysis. In rats pretreated with vehicle, plantar incision caused robust hyperalgesia, up-regulated 36 genes and downregulated 90 genes in dorsal root ganglia one day after plantar incision. Capsaicin pretreatment attenuated pain behaviors, caused localized denervation of the dermis and epidermis, and prevented the incision-induced changes in 99 of 126 genes. The pathway analyses showed altered gene networks related to increased pro-inflammatory and decreased anti-inflammatory responses in dorsal root ganglia. Insulin-like growth factor signaling was identified as one of the major gene networks involved in the development of incisional pain. Expression of insulin-like growth factor -2 and IGFBP6 in dorsal root ganglia were independently validated with quantitative real-time polymerase chain reaction. We discovered a distinct subset of dorsal root ganglia genes and three key signaling pathways that are altered 24 h after plantar incision but are unchanged when incision was made after capsaicin infiltration in the skin. Further exploration of molecular mechanisms of incisional pain may yield novel therapeutic targets.

Keywords

Dorsal root ganglia, insulin-like growth factor, incisional pain, postoperative pain, transcriptome

Date Received: 27 May 2020 Date Received: 22 July 2020; accepted: 23 July 2020

Introduction

Management of acute incisional pain is an essential component of perioperative care. Approximately 234 million major surgical procedures are performed every year worldwide,¹ and approximately 20% of these are performed in the United States alone.² Uncontrolled or postoperative pain is reported by approximately 50% of surgical patients.^{3,4} Opioids are the mainstay for perioperative pain management. However, they produce an array of harmful side effects including nausea,⁵ tolerance (requirement of an increased dose for analgesia),⁶ hyperalgesia,⁷ constipation,⁵ ileus,⁸ urinary retention,⁸ respiratory depression,⁵ and death in overdose cases.⁹

¹Department of Pediatrics, School of Medicine, University of Minnesota, Minneapolis, MN, USA

²Department of Anesthesiology, School of Medicine, University of Minnesota, Minneapolis, MN, USA

³Department of Diagnostic and Biological Sciences, School of Dentistry, University of Minnesota, Minneapolis, MN, USA

⁴Informatics Institute, University of Minnesota, Minneapolis, MN, USA

*The first two authors contributed equally to this study.

Corresponding Author:

Ratan K Banik, Department of Anesthesiology, University of Minnesota, Twin Cities Campus, B515 Mayo Memorial Building, 420 Delaware Street S. E., MMC 294, Minneapolis, MN 55455, USA.
Email: rkbantik@umn.edu



Importantly, patients receiving an opioid prescription after surgery were 44% more likely to become long-term opioid users compared with those who did not receive opioids.^{10,11} Thus, there is a need to develop non-opioid approaches for managing incisional pain.

The development of non-opioid therapies for incisional pain requires a comprehensive understanding of the underlying molecular mechanisms. For peripheral mechanisms of incisional pain, it is critical to identify molecular changes in primary afferent neurons that innervate incised tissues. In this regard, next-generation high-throughput sequencing (NGS) technology have been used to evaluate the gene expression profiles in several preclinical pain models^{12–16} but not in incisional pain. Because sensory neurons from different tissues respond uniquely to injury,^{17–19} it is necessary to assess incisional pain-related changes in gene expression.

A rat model of incisional pain has been extensively characterized, which includes behavioral phenotypes, nociceptor sensitization, and pharmacologic modulation.^{20–25} Additionally, our lab and others have reported that intra-plantar infiltration of capsaicin attenuates spontaneous pain behaviors and heat hyperalgesia.^{26,27} This phenomenon provides a unique opportunity to identify neural transcriptomes that are specifically induced during incisional pain. For example, incision-induced gene regulatory changes that are sensitive to capsaicin pretreatment are likely involved in the development of pain after incision, whereas those which are insensitive to capsaicin pretreatment are likely involved in processes unrelated to pain.

We, therefore, determined the effect of incisional pain on the transcriptional profile of the dorsal root ganglia (DRG) by performing whole-transcriptome next-generation RNA sequencing. We hypothesized that the acute incisional injury will dramatically alter gene transcription in the rat DRGs, and that we would identify novel pain pathways, which may yield novel therapeutic targets.

Methods

Animals

Adult male Sprague–Dawley rats (250–300 g) purchased from Charles River (USA) were used in this study. Two rats were housed together in one Plexiglass cage and all animals were maintained on a 12 h light/dark cycle with free access to food and water. All procedures were approved by the Institutional Animal Care and Use Committees at the University of Minnesota.

Surgical procedures

Rats were anesthetized with isoflurane for intra-plantar injection of capsaicin, vehicle, and plantar incision.

Briefly, rats were placed in an induction chamber using 5% isoflurane in room air followed by 2% to 3% isoflurane via a nose cone after loss of the righting reflex. Once adequately anesthetized, the intended surgical site for incision (mid-plantar region of the right hind paw) was infiltrated subcutaneously with 200 μ L of either 1% capsaicin (10 mg/mL) or vehicle (80% saline, 10% ethanol, 10% Tween-80 (Sigma-Aldrich, St. Louis, MO)) using a 1 mL syringe with a 25 G needle. Surgery consisted of a 20 mm longitudinal incision made through the skin and fascia of the plantar hind paw as previously described.^{23,25} The flexor digitorum brevis muscle was then elevated, stressed, and incised longitudinally with the muscle origin and insertion remaining intact. The skin was closed with two mattress 5–0 silk sutures. Animals were housed on soft bedding and allowed to recover. Sutures were removed on the third post-operative day. Sham control rats underwent anesthesia but not surgical incision.

Measurement of spontaneous foot lifting behaviors

Spontaneous foot lifting (SFL) was used as a measure of spontaneous pain as described previously.²⁵ Rats were pre-treated with capsaicin (n = 5) or vehicle (n = 6) for 30 min prior to surgical incision. Frequency and duration of SFL were obtained longitudinally at 3 h and at 1, 2, 3, 4, 5, 7, 9, and 16 days after surgery. In brief, animals were placed in individual Plexiglass chambers on a mesh floor above an angled mirror and habituated for 30 min to minimize exploratory behavior during the assessment period. Spontaneous, rapid lifting of the incised hind paw was recorded with a hand tally counter and the duration of prolonged (>1 s) paw elevation was recorded with a stopwatch. Each rat was tested over four 5-min periods with 5 to 10 min resting intervals between each assessment. The sum frequency of SFL and sum duration of paw lifts were determined for each rat.

Measurement of hyperalgesia to heat

Sensitivity to heat was determined by measuring paw withdrawal latencies to heat (PWL). The same rats tested for SFL were used. PWL were determined 3, 2, and 1 day before surgery and at 3 h and 1, 2, 3, 4, 5, 7, 9, and 16 days after surgery. Rats were placed under Plexiglass boxes (23.6 cm \times 13.8 cm \times 13.7 cm) on a tempered glass floor (3-mm thickness) that was maintained at 30 °C and allowed to acclimate for 20 min. A focused radiant heat source (50 W projector lamp with an aperture diameter of 6 mm) underneath the glass floor was aimed at the plantar surface of the injured paw and withdrawal latencies were determined. PWLs were measured to the nearest 0.01 s by an automated system. The intensity of the heat was adjusted to produce withdrawal

latencies in normal, naive rats of 10 to 12 s. Mean PWL for each rat was obtained from three trials with a 5-min inter-stimulus interval between trials. The experimenter collecting all behavioral data was blinded to treatment condition of rats; however, blinding was limited due to distinct changes in PWL due to capsaicin pretreatment.

Measurement of mechanical hyperalgesia

The same rats tested for SFL were used to test for mechanical paw withdrawal (PWT) 3, 2, and 1 day before surgery and at 3 h and 1, 2, 3, 4, 5, 7, 9, and 16 days after surgery. Rats were placed in individual Plexiglass chambers on a mesh floor and allowed to habituate for 30 min. Mechanical PWT was determined using an electronic von Frey aesthesiometer (IITC Life Science, Woodland Hills, CA). This consists of a hand-held force transducer with a series of rigidity-graded, attachable 0.8 mm polypropylene tips. Starting with the least rigid tip, force was transversely applied for to the mid-plantar surface of the hind paw (adjacent to the site of surgical injury) until the occurrence of a rapid paw withdrawal response. Stimuli were applied for 2 to 3 s with an inter-stimulus interval of 5 min. The second and third trials were conducted using the tip that was two grades lower than the tip which elicited the first withdrawal response. Withdrawal thresholds (g) were expressed as the mean from three trials.

Immunohistochemistry and confocal laser scanning microscopy

The epidermal and dermal nerve fibers were assessed by immunohistochemistry as previously described by our group.^{28,29} In brief, rats were anesthetized with isoflurane as described above, and treated with 1% capsaicin (n = 3) or vehicle (n = 3) 30 min prior to the surgical incision. After 24 h, rats were euthanized with euthasol (390 mg/mL Pentobarbital), and after no righting reflex, 200 μ L of Zamboni's fixative was injected into the hind paw. The hind paw was removed and placed in Zamboni's fixative at 4°C for 24 h, then 20% sucrose at 4°C for 24 h. A 3-mm punch biopsy tool was used to remove tissue from the edge of the incision. For sectioning, tissues were immersed in OCT mounting medium (Electron Microscopy Sciences, Hatfield, PA) frozen on a cryo-microtome and cut into 50 μ m thick sections. Free floating tissue sections were incubated 1 h in blocking buffer (10% normal donkey serum/PBS/0.1% Triton X-100), then overnight in antibody buffer (3% normal donkey serum/PBS/0.1% Triton X-100) containing DAPI, rabbit anti-advillin, and goat anti-collagen type IV. Sections were rinsed with antibody buffer three times, 1 h each time, and then incubated for an additional day in Cy5-conjugated donkey anti-goat and Cy3-

conjugated donkey anti-rabbit secondary antibodies. Sections were rinsed in antibody buffer three times, 1 h each time, and then mounted in hot liquid noble agar onto 22 mm² coverslips that were dehydrated in 95%, 100% ethanol, and cleared with 100% methyl salicylate for 30 min each before placing in DPX mounting medium on slides. Fluorescent images were captured using a Nikon Ti2 laser scanning confocal microscope equipped with an oil immersion objective using Nikon Elements software. Digitized images were collected in successive frames of 0.5- μ m serial optical sections (z-series) throughout the thickness of the sections and flattened into a single image. The immunostaining of type IV collagen was used to localize the dermo-epidermal boundary.

RNA sequencing

Thirty min prior to incisional surgery, rats were treated either with (n = 4) or without (n = 4) capsaicin (see above). The L4–L6 DRGs collected from control (sham) rats (n = 4) and rats at 24 h after plantar incision. Surgery was carried out in the afternoon between 3 and 5 pm. Total RNA isolated from DRGs (RNAqueous RNA isolation kit, Life Technologies Inc., Carlsbad, CA) were quantified and qualified by RiboGreen RNA quantification (Invitrogen, Carlsbad, CA) and an Agilent 2100 Bioanalyzer (Agilent Inc., Santa Clara, CA). Median RNA integrity score in samples was 7.9 (interquartile range, 7.825–8.275). The median mass input was 5698 ng (Supplemental Figure 3). A total of 100 ng of RNA samples with RIN values \geq 8.0 were used for library construction using a TruSeq RNA v2 kit (Illumina, San Diego, CA). Libraries were size-selected \sim 200-bp inserts and sequenced as a 50-bp pair end using the HiSeq2000 (Agilent Inc.).

Bioinformatics

2 \times 50 bp FastQ paired end reads (n = 18.8 Million average per sample) were trimmed using Trimmomatic (v 0.33) enabled with the optional “-q” option; 3 bp sliding-window trimming from 3' end requiring minimum Q30. Quality control on raw sequence data for each sample were performed with FastQC. Read mapping was performed via Hisat2³⁰ (v2.1.0) using the rat genome (rn6) as reference. Gene quantification was done via Feature Counts for raw read counts. Differentially expressed genes were identified using the edgeR^{31,32} (negative binomial) feature in CLCGWB (Qiagen, Redwood city, CA) using raw read counts. We filtered the generated list based on a minimum 1.5 \times Absolute Fold Change and false discovery rate corrected $p < 0.05$.

Gene networks mapping by Ingenuity Pathway Analysis

The differentially expressed transcripts were uploaded to Ingenuity Pathway Analysis (IPA; Ingenuity Systems, Redwood City, CA) to identify regulatory networks operant in rat DRGs. IPA provides an extensive description of biological processes, molecular functions, and cellular components to test for enrichment of associated gene.³³ Analysis was restricted to 126 genes, whose expression was changed in the incised rats. Moreover, *p* value is calculated by determining the probability that a disease or biological function assigned to the data. To show the connectivity between genes, and to classify them according to the molecular mechanisms, differentially expressed genes are categorized by Medical Subject headings terms and proprietary ontology. The significance of the association is measured by the ratio of the number of genes from the dataset that map to the canonical pathway divided by the total number of known genes in that pathway.

Quantitative real-time PCR

The quantitative real-time PCR (qPCR) experiments were carried out with biological replicates (*n* = 3–5/group). In brief, 1 µg of total RNA was used to generate complementary DNA (cDNA; High Capacity cDNA reverse transcription kit; Life Technologies). Gene expressions were quantified using TaqMan Gene Expression Assay probes (Applied Biosystems, Foster City, CA) and a DNA analyzer (Quant Studio, Applied Biosystems Inc.). Samples were analyzed in technical duplicates. Fold changes are means of duplicates, normalized to β -actin (internal loading control). Taqman gene expression assays include Rn00565371_m1 (IGFBP6), Rn01454518_m1 (IGF2), and Rn00667869_m1 (Actb).

Statistical analysis

Two-way analyses of variance (ANOVAs) with repeated measures were used to compare differences in the frequency and duration of SFL, PWT, and PWL. Post hoc comparisons (Bonferroni) were used to determine differences between vehicle and capsaicin-treated groups at specific time points. For qPCR validation, interactions were analyzed using ANOVA or unpaired *t*-test for differences between groups. α was set at <0.05. For IPA comparison analysis, Fisher's exact test was used to calculate a *p*-value for the association among genes in the data sets, pathways, and functions. The generated diseases or functional annotations or upstream regulators were ranked by the activation *z* score. An absolute *z* score of more than 2 was considered as significant. All values are expressed as means \pm SDs

Results

Intra-plantar capsaicin infiltration attenuated pain behaviors after plantar incision and reduced innervation in the dermis and epidermis

Following plantar incision, rats exhibited spontaneous pain-like behaviors and hypersensitivity to mechanical and heat stimuli that persisted for three to nine days (Figure 1(a) to (d)). Compared to vehicle (*n* = 6), intra-plantar injection with 1% capsaicin (*n* = 5) 30 min before surgical incision significantly attenuated SFL frequency ($F_{2,11} = 2.0$, *p* = 0.059); duration ($F_{2,11} = 2.20$, *p* = 0.037) and prevented the development of both mechanical ($F_{2,11} = 11.2$, *p* < 0.0001) and heat hyperalgesia ($F_{2,11} = 28.9$, *p* < 0.0001). Epidermal and dermal innervation following vehicle or 1% capsaicin infiltration was examined in rats 24 h following plantar incision. Representative confocal images of immune-stained skin from each of these groups are shown in Figure 1(e) and (f). A complete loss of epidermal and dermal nerve fibers were observed in hind paw skin pretreated with capsaicin (Figure 1(f), arrow).

Identification of differentially expressed genes in DRGs after plantar incision

To determine the transcriptomic changes in the primary afferent neurons that occur following plantar incision, we sequenced DRG transcripts using NGS. Three groups of rats were used such as control (sham) rats, rats with plantar incision, and rats treated with intra-plantar capsaicin 30 min prior to plantar incision. This approach allowed us to identify genes that are potentially involved in incisional pain behaviors because intra-plantar capsaicin completely denervated epidermal and dermal nerves around the incision and abolished hyperalgesia and SFL behaviors (Figure 1).

Using selection criteria that include an absolute fold change $\geq 1.5\times$, *p* < 0.05, and a false discovery rate < 0.05, 126 genes were identified in the incised compared to sham group, including 36 that were up-regulated (incision vs. control; Table 1) and 90 that were down-regulated (incision vs. control; Table 2). Capsaicin pretreatment prevented transcriptional changes in 99 of 126 genes, including 20 of the upregulated and 79 of the down-regulated genes (Figure 2(a) and (b), Inci vs. Inci + Cap). These genes are displayed in the heat map (Figure 2(a)) to illustrate the degree of reproducibility among biological replicates. IPA mapped these genes onto specific diseases and biological functions (Figure 2(c)). Compared to sham control (Cntl) group, incised groups showed changes in the expression of genes associated with increased morbidity, organismal death, and decreased growth and differentiation (Figure 2(c), Inci).

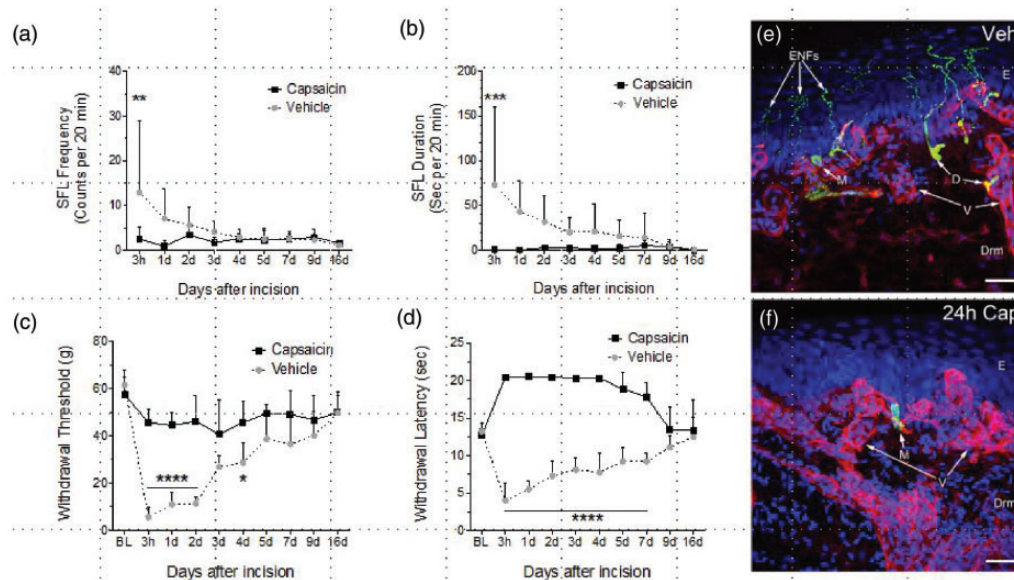


Figure 1. Capsaicin pretreatment attenuates the development of pain-like behaviors 24 h after plantar incision. The frequency (a) and duration (b) of plantar incision-induced spontaneous foot lifting behaviors (see methods) as well as mechanical (c) and heat (d) hyperalgesia were decreased in capsaicin-treated groups compared to vehicle-treated rats. The capsaicin pretreatment completely abolished epidermal and dermal nerves (f) compared with vehicle treated (e) rats 24 h after incision. In immunohistochemistry experiments, the tissue cryosections were immune-stained with anti-advillin antibody to label nerve fibers (green) and with anti-collagen type IV antibody to label basement membranes (red). Yellow indicates colocalization of the two antibodies. Cell nuclei were labeled with DAPI (blue). Each image in this figure represents a maximum projection of an image stack captured as 0.5 μm optical slices through the immune-stained tissue. Merkel cells (M) were unchanged with capsaicin treatment. No changes were evident in blood vessels (V) in the dermis. E indicates the location of epidermis and Drm indicates dermis. Scale bar = 50 microns.

These changes in gene expression were abrogated with capsaicin pretreatment (Figure 2(c), Inci+Cap).

Regulatory networks involved in plantar incision-induced pain behaviors

To identify the regulatory networks involved in the development of incisional pain, IPA was used to annotate these genes onto known functional gene networks. Specific analysis of DRG genes, which are altered 24 h after plantar incision but unchanged when rats were pretreated with 1% capsaicin in skin, predicted lower activity of CCAAT/enhancer-binding protein beta (CEBPB), forkhead box M1 (FOXM1), prostaglandin E(2) receptor (PTGER2), and BRD4 (Figure 3). These changes are associated with reduced cell proliferation, increased bleeding, and organismal death (Figure 3).

Changes in inflammatory genes following plantar incision

We have identified that plantar incision induces the expression of DRG genes that regulates inflammatory processes. In particular, markedly increased expression of IFIT1B (~50-fold), IL2Ra, CD274 were predictive of increased toll-like receptor 9 (TLR9) signaling (Figure 4 (a)), which was attenuated with capsaicin pretreatment

(Figure 4(b)). Conversely, reduced expression of EDNRB, EMP2, and FBN1 coupled with increased expression of INHBA and Sult1a1 were indicative of reduced IL10Ra signaling (Figure 4(c)), which was attenuated by capsaicin pretreatment (Figure 4(d)). These results suggest plantar incision produces a change in genes leading to increased pro-inflammatory responses and decreased anti-inflammatory responses in the DRG.

Insulin-like growth factor signaling pathway is involved in incisional pain

The analysis of differentially expressed DRG genes showed evidence of reduced insulin-like growth factor (IGF) signaling pathway with downregulation of IGF1, IGFBP3, MPZ, and COL1A1 accompanied by upregulation of IGF2 and IGFBP6 (Figure 5(a)). Capsaicin pretreatment prevented the upregulation of IGF2 and IGFBP6 (Figure 5(b)). Further, IPA linked these transcriptional changes to reduced PI3K and ERK signaling, leading to altered expression of ERK target genes (Figure 5(c)). To independently validate NGS data, expression of IGF2 and IGFBP6 were quantified by qPCR using a different set of biological replicates. The significant upregulation of IGF2 and IGFBP6 were confirmed in the DRGs from incised rats, which

Table 1. List of upregulated genes in the dorsal root ganglia after plantar incision.

Gene Name	Gene symbol	log2(Fold change)	Location	Type(s)
Germ cell-less homolog 1 (Drosophila)-like	LOC302576	53.20	Other	Other
Interferon-induced protein with tetratricopeptide repeats 1B	Ifit1	50.10	Cytoplasm	Other
Inhibin subunit beta A	Inhba	42.46	Extracellular space	Growth factor
Interleukin 2 receptor subunit alpha	Il2ra	34.32	Plasma membrane	Transmembrane receptor
Chitinase domain containing 1	Chid1	27.50	Extracellular space	Other
Aquaporin 4	Aqp4	13.53	Plasma membrane	Transporter
Exocyst complex component 7	Exoc7	9.69	Cytoplasm	Transporter
Urocortin	Ucn	9.19	Extracellular space	Other
CD300c molecule	RGD1559482	6.24	Plasma membrane	Transmembrane receptor
Solute carrier family 22 member 6	Slc22a6	4.11	Plasma membrane	Transporter
ALK and LTK Ligand 2	Fam150b	4.06	Extracellular space	Other
Coiled-coil domain containing 153	Ccdc153	3.70	Other	Other
C-X-C motif chemokine ligand 13	Cxcl13	3.56	Extracellular space	Cytokine
Prostaglandin D2 synthase	Ptgds	3.27	Cytoplasm	Enzyme
Troponin T2, cardiac type	Tnnt2	3.09	Cytoplasm	Other
Insulin-like growth factor 2	Igf2	2.97	Extracellular space	Growth factor
Aldehyde dehydrogenase 1 family member A2	Aldh1a2	2.92	Cytoplasm	Enzyme
Hematopoietic SH2 domain containing	Hsh2d	2.88	Cytoplasm	Other
Solute carrier family 22 member 8	Slc22a8	2.69	Plasma membrane	Transporter
Prepronociceptin	Pnoc	2.58	Extracellular space	Other
Mitochondria localized glutamic acid-rich protein	Mgap	2.52	Cytoplasm	Other
Solute carrier family 6 member 13	Slc6a13	2.52	Plasma membrane	Transporter
Ankyrin repeat domain 33B	Ankrd33b	2.27	Other	Other
Gap junction protein beta 6	Gjb6	2.14	Plasma membrane	Transporter
Astacin-like metalloendopeptidase	Astl	2.09	Cytoplasm	Peptidase
Solute carrier family 16 member 11	Slc16a11	1.99	Cytoplasm	Transporter
Tripartite motif containing 45	Trim45	1.95	Cytoplasm	Other
Myomesin 2	Myom2	1.90	Cytoplasm	Other
Activating transcription factor 3	Atf3	1.83	Nucleus	Transcription regulator
Sulfotransferase family 1A, phenol-preferring, member 1	Sult1a1	1.70	Cytoplasm	Enzyme
CD274 molecule	Cd274	1.66	Plasma membrane	Enzyme
Insulin-like growth factor binding protein 6	Igfbp6	1.65	Extracellular space	Other
Serine peptidase inhibitor, Kunitz type 2	Spint2	1.59	Extracellular space	Other
Cholinergic receptor nicotinic alpha 6 subunit	Chrna6	1.55	Plasma membrane	Transmembrane receptor
RNA binding motif protein 3	Rbm3	1.52	Cytoplasm	Other

were prevented with capsaicin pretreatment (Figure 5(d); IGF2: $F_{2,10} = 16.99$, $p = 0.0006$; IGFBP6: $F_{2,11} = 26.22$, $p < 0.0001$).

Plantar incision-induced changes in genes not related to pain

IPA annotation of 27 DRG genes that are not influenced by capsaicin pretreatment in plantar skin (Figure 2(b)) revealed changes in cellular responses including decreased recruitment of myeloid cells, cell movement,

and cellular necrotic death. These effects were accompanied by increased vascularization and organismal death (Figure 6). These responses may have a role in surgical injury and repair and unlikely to be involved in the pain processing after incision.

Discussion

Our study is the first genome-wide transcriptional profiling of DRG tissues in a rat model of incisional pain. We identified changes in gene expression in the DRG

Table 2. List of downregulated genes in the dorsal root ganglia after plantar incision.

Gene Name	Gene symbol	log ₂ (Fold change)	Location	Type(s)
Myosin light chain 1	Myl1	-6.00	Cytoplasm	Other
H19 imprinted maternally expressed transcript	H19	-4.32	Cytoplasm	Other
DNA topoisomerase II alpha	Top2a	-4.05	Nucleus	Enzyme
Collagen type II alpha 1 chain	Col2a1	-3.76	Extracellular space	Other
Centromere protein T	Cenpt	-3.59	Cytoplasm	Transcription regulator
Ribonucleotide reductase regulatory subunit M2	Rrm2	-3.46	Nucleus	Enzyme
BUB1 mitotic checkpoint serine/threonine kinase B	Bub1b	-3.42	Nucleus	Kinase
Family with sequence similarity 84 member A	Fam84a	-3.37	Other	Other
Integrin subunit beta 3	Itgb3	-3.33	Plasma membrane	Transmembrane receptor
Syntrophin gamma 2	Sntg2	-2.98	Plasma membrane	Other
Kinesin family member 18B	Kif18b	-2.95	Cytoplasm	Other
Beta-1,4-N-acetyl-galactosaminyltransferase 3	B4galnt3	-2.85	Cytoplasm	Enzyme
CIq and TNF-related 6	CIqtnf6	-2.81	Extracellular space	Other
Cyclin B2	Ccnb2	-2.76	Cytoplasm	Other
Centromere protein F	Cenpf	-2.76	Nucleus	Other
Protein regulator of cytokinesis 1	Prc1	-2.71	Nucleus	Other
CD93 molecule	Cd93	-2.56	Plasma membrane	Other
Grainyhead like transcription factor 3	Grhl3	-2.36	Nucleus	Transcription regulator
Insulin-like growth factor 1	Igf1	-2.33	Extracellular space	Growth factor
Collagen type III alpha 1 chain	Col3a1	-2.31	Extracellular space	Other
Collagen type XI alpha 1 chain	Col11a1	-2.30	Extracellular space	Other
Apelin receptor	Aplnr	-2.23	Plasma membrane	G-protein-coupled receptor
Ewing sarcoma breakpoint region 1	Ewsr1	-2.21	Nucleus	Other
Periostin	Postn	-2.21	Extracellular space	Other
Nucleolar and spindle-associated protein 1	Nusap1	-2.19	Nucleus	Other
Collagen type VIII alpha 1 chain	Col8a1	-2.18	Extracellular space	Other
Chromosome 2 open reading frame 40	RGD1305645	-2.15	Extracellular space	Other
Collagen type I alpha 1 chain	Col1a1	-2.13	Extracellular space	Other
Tenascin C	Tnc	-2.11	Extracellular space	Other
NUF2 component of NDC80 kinetochore complex	Nuf2	-2.08	Nucleus	Other
Collagen type XIV alpha 1 chain	Col14a1	-2.07	Extracellular space	Other
Fibrillin 2	Fbn2	-2.05	Extracellular space	Other
Transmembrane protein 26	Tmem26	-2.04	Other	Other
Myosin heavy chain 6	Myh6	-2.01	Cytoplasm	Enzyme
RAB7B, member RAS oncogene family	Rab7b	-1.99	Cytoplasm	Peptidase
EMI domain containing 1	Emid1	-1.97	Extracellular space	Other
Secreted frizzled-related protein 4	Sfrp4	-1.96	Plasma membrane	Transmembrane receptor
Kirre-like nephrin family adhesion molecule 1	Kirrel	-1.91	Plasma membrane	Other
Minichromosome maintenance complex component 6	Mcm6	-1.88	Nucleus	Enzyme
Feline leukemia virus subgroup C cellular receptor family member 2	Flvcr2	-1.84	Plasma membrane	Transporter
Peripheral myelin protein 2	Pmp2	-1.80	Cytoplasm	Other
Niban apoptosis regulator 1	Fam129a	-1.77	Cytoplasm	Other
Acyl-CoA thioesterase 1	Acot1	-1.75	Cytoplasm	Enzyme
Collagen type XXVII alpha 1 chain	Col27a1	-1.73	Extracellular space	Other
Collagen type IV alpha 1 chain	Col4a1	-1.73	Extracellular space	Other
ETS transcription factor ELK1	Elk1	-1.72	Nucleus	Transcription regulator
Collagen type V alpha 2 chain	Col5a2	-1.68	Extracellular space	Other

(continued)

Table 2. Continued.

Gene Name	Gene symbol	log ₂ (Fold change)	Location	Type(s)
POU class 3 homeobox 2	Pou3f2	-1.68	Nucleus	Transcription regulator
Leucine-rich repeat containing G protein-coupled receptor 5	Lgr5	-1.67	Plasma membrane	Transmembrane receptor
Fibrillin 1	Fbn1	-1.67	Extracellular space	Other
Nidogen 2	Nid2	-1.66	Extracellular space	Other
Pyridine nucleotide-disulphide oxidoreductase domain 2	Pyroxd2	-1.66	Other	Other
TLR4 interactor with leucine-rich repeats	Tril	-1.65	Other	Other
Dedicator of cytokinesis 1	Dock1	-1.64	Cytoplasm	Other
Transmembrane serine protease 5	Tmprss5	-1.64	Plasma membrane	Peptidase
Fatty acid desaturase 2	Fads2	-1.63	Plasma membrane	Enzyme
Bone morphogenetic protein 1	Bmp1	-1.61	Extracellular space	Peptidase
Protein phosphatase 1 regulatory inhibitor subunit 14C	Ppp1r14c	-1.60	Cytoplasm	Other
KDEL motif containing 1	Kdelc1	-1.60	Cytoplasm	Enzyme
Myelin protein zero	Mpz	-1.60	Plasma membrane	Other
Sclerostin domain containing 1	Sostdc1	-1.59	Extracellular space	Growth factor
Thrombospondin 2	Thbs2	-1.59	Extracellular space	Other
Laminin subunit alpha 4	Lama4	-1.59	Extracellular space	Enzyme
C-X-C motif chemokine receptor 4	Cxcr4	-1.59	Plasma membrane	G-protein-coupled receptor
Protein tyrosine phosphatase receptor type Z1	Ptprz1	-1.58	Plasma membrane	Phosphatase
Transforming growth factor beta receptor 3	Tgfr3	-1.58	Plasma membrane	Kinase
Cysteine and tyrosine rich 1	Cypr1	-1.58	Other	Other
Glycerophosphodiester phosphodiesterase domain containing 2	Gdpd2	-1.58	Plasma membrane	Enzyme
Fms-related tyrosine kinase 1	Flt1	-1.58	Plasma membrane	Kinase
Uncharacterized LOC100912041	LOC100912041	-1.58	Plasma membrane	Transmembrane receptor
Sortilin-related VPS10 domain containing receptor 2	Sorcs2	-1.58	Plasma membrane	Transporter
Endothelin receptor type B	Ednrb	-1.58	Plasma membrane	G-protein-coupled receptor
UDP glycosyltransferase 8	Ugt8	-1.57	Cytoplasm	Enzyme
ADAM metallopeptidase with thrombospondin type 1 motif 5	Adamts5	-1.57	Extracellular space	Peptidase
Collagen type V alpha 1 chain	Col5a1	-1.57	Extracellular space	Other
Chondromodulin	Lect1	-1.57	Extracellular space	Other
Plexin B3	Plxnb3	-1.56	Plasma membrane	Transmembrane receptor
Eadherin EGF LAG seven-pass G-type receptor 2	Celsr2	-1.56	Plasma membrane	G-protein-coupled receptor
ANTXR cell adhesion molecule 1	Antxr1	-1.56	Plasma membrane	Transmembrane receptor
SLIT- and NTRK-like family member 2	Slitrk2	-1.54	Plasma membrane	Other
Myelin-associated glycoprotein	Mag	-1.54	Plasma membrane	Other
Epithelial membrane protein 2	Emp2	-1.54	Plasma membrane	Other
nudE neurodevelopment protein 1	Nde1	-1.53	Nucleus	Other
Sphingosine kinase 1	Sphk1	-1.52	Cytoplasm	Kinase
Growth arrest specific 7	Gas7	-1.52	Cytoplasm	Transcription regulator
Insulin-like growth factor binding protein 3	Igfbp3	-1.52	Extracellular space	Other
PDZ domain containing 2	Pdzd2	-1.52	Plasma membrane	Other
Leucine-rich repeat transmembrane neuronal 1	LRRTM1	-1.51	Plasma membrane	Other
Erb-b2 receptor tyrosine kinase 3	ErbB3	-1.51	Plasma membrane	Kinase
Podoplanin	Pdpn	-1.50	Plasma membrane	Other
Peroxidasin	Pxdn	-1.50	Extracellular space	Enzyme

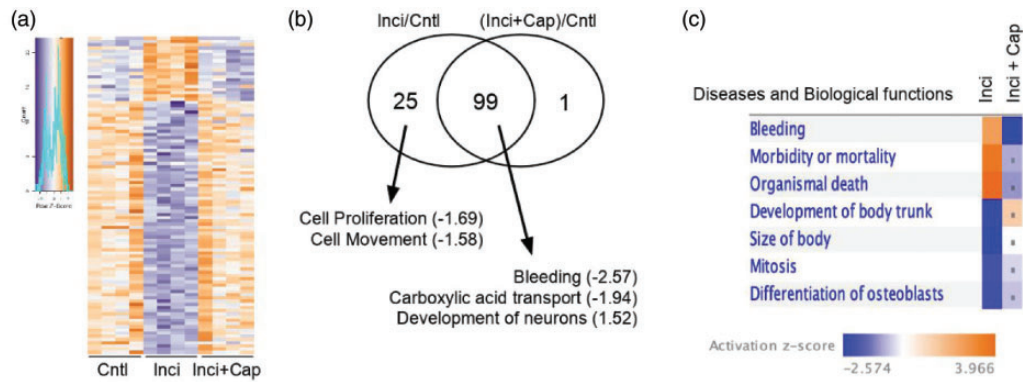


Figure 2. The global transcriptome analysis on rat dorsal root ganglia (DRG) identifies the genes that are significantly altered in one day after plantar incision. The infiltration of capsaicin 30 min prior to surgical incision completely prevented incision-induced transcriptional changes in 99 of 126 (79%) genes; shown in a heat map (a). Each line represents a gene across three groups ($n = 4/\text{group}$). Shades of blue and orange indicate negative and positive z-scores, respectively. (b) Venn diagram showing altered functions associated with two distinct groups of genes. Both groups underwent plantar incision but one was pretreated with capsaicin (inci + cap) and the other was not (Inci). Values in parentheses indicate z-score where negative and positive values predict inhibition and activation, respectively. (c) The differentially expressed genes from Inci + cap and Inci were compared by IPA. The top diseases and biological functions were related to “mortality morbidity” and “organismal death”. Dots indicate z-score < 2.0.

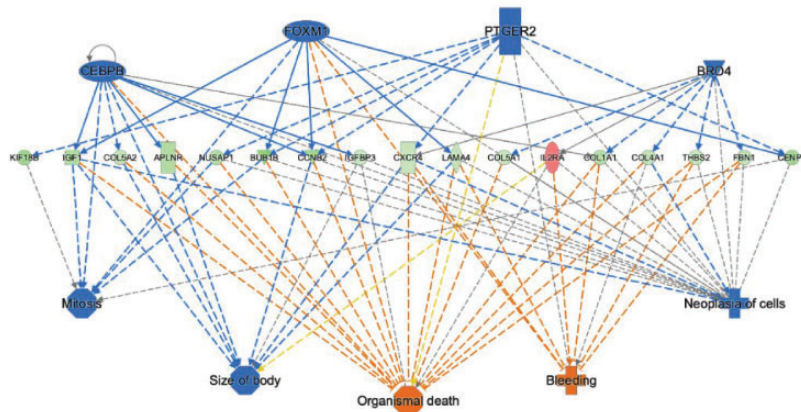


Figure 3. Altered regulatory networks and associated downstream effects in DRG following plantar incision. Analysis of differentially expressed genes indicated reduced activity of CEBPB, FOXMI, PTGER2, and BRD4 regulatory factors (z-score < -2.0), leading to increased risk organismal mortality accompanied by decreased mitosis and tissue size. Legends: Upregulation: red; downregulation: green; predicted inhibition: blue; predicted activation: orange.

at one day after plantar incision, a time point at which pain behaviors were most prominent. The skin infiltration of capsaicin 30 min prior to surgical incision attenuated incision-induced pain behaviors, completely denervated the epidermis and dermis around the incision, and prevented incision-induced transcriptional changes in 99 of 126 DRG genes (79%), suggesting the majority of these transcriptional changes were related to post-operative pain development. These findings highlight novel gene networks associated post-operative pain including neuro-inflammation and the IGF signaling.

Global analysis of transcriptome in rat DRG following plantar incision

Plantar incision alone induced 36 upregulated and 90 downregulated genes in L4–L6 DRGs. These results are significant and robust compared to a previous polymerase chain reaction array study by Spofford and Brennan,³⁴ who showed few changes in gene expression in DRGs using similar incision model.³⁴ The disparate results were likely due to the use of different techniques. The qPCR approach by Spofford and Brennan³⁴ is limited to measuring single transcripts and requires priori

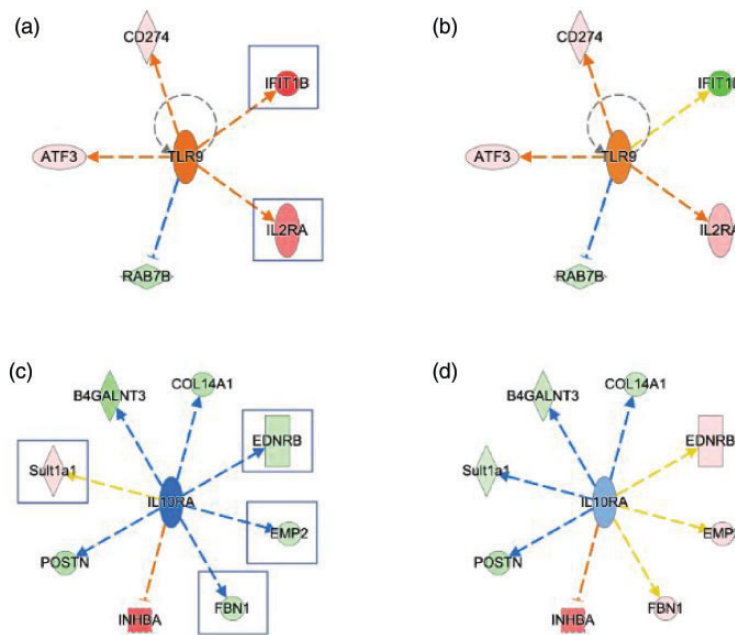


Figure 4. Changes in gene expression leading to increased pro-inflammatory and decreased anti-inflammatory responses in DRG following plantar incision (a, b). IPA predicted increased toll-like receptor 9 (TLR9) activity due to increased expression of IFIT1B and IL2RA (a, boxed). Capsaicin pretreatment (b) diminished these transcriptional responses. (c–d) Altered gene expression suggests a decreased anti-inflammation in incision group (c), which were not altered with capsaicin pretreatment (d).

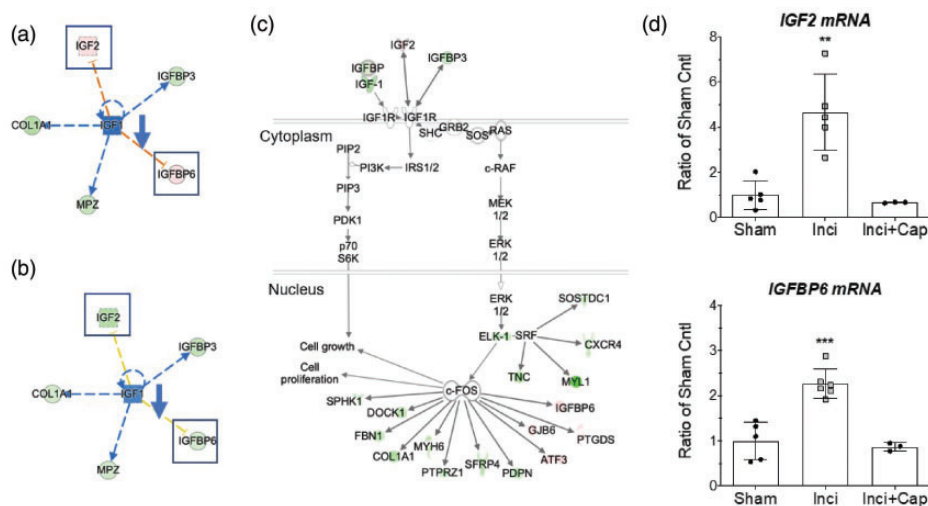


Figure 5. Altered IGF1 signaling in DRG of rats after plantar incision. (a, b) IGF1 gene networks showing altered expression level in incision group (a) and incision with capsaicin pretreated group (b). Boxed genes indicate those that responded to capsaicin treatment. (c) IPA mapped differentially expressed genes onto IGF1 canonical pathway suggesting reduced cell growth and proliferation. (d) qPCR validation of IGF2 and IGFBP6 in DRG. Values are mean \pm SD, $n = 3-6$ /group, t -test, $**p < 0.01$, $***p < 0.001$.

known gene targets. In contrast, RNA Seq, used in the present study, is an agnostic and more comprehensive approach that covers the entire transcriptome (>26,000 gene loci) present in DRGs. Moreover, this approach allows a better resolution of complex nature of the transcriptome including a detailed and quantitative measure

of gene expression. Notably, the number of downregulated genes much greater than the number of upregulated genes; however, the fold change in expression for the upregulated genes was markedly higher than that for the downregulated genes (Figure 7, Tables 1 and 2). The higher number of downregulated versus upregulated

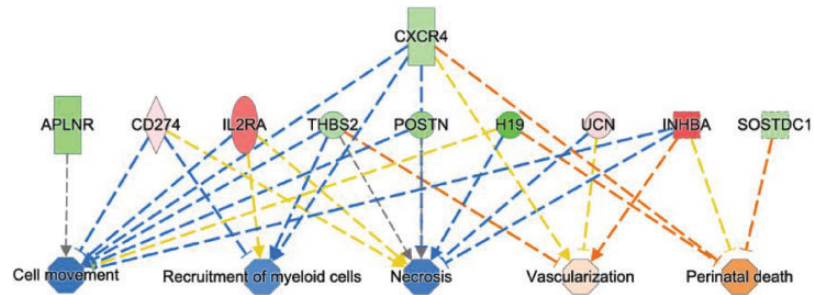


Figure 6. Functional annotation of DRG genes that were regulated by plantar incision but were not influenced by the capsaicin pretreatment. IPA mapped functions of these 25 genes indicating reduced cell movement, recruitment of myeloid cells, and necrosis as well as increased vascularization and risk of perinatal death.

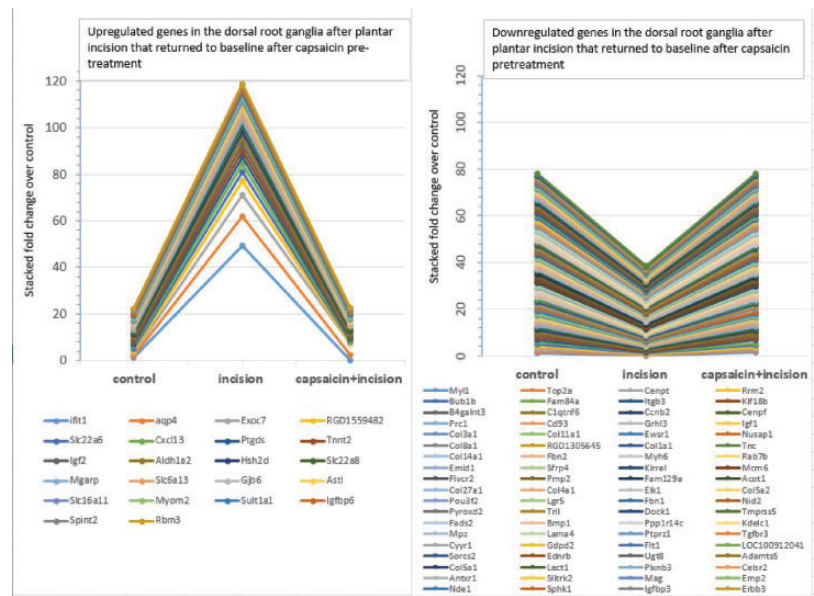


Figure 7. Data presented in figure 2 are shown as stacked percentage chart showing degree of expression changes relative to the total changes in gene expression in dorsal root ganglia (DRG) following plantar incision. Left: upregulated genes; Right: downregulated genes.

transcripts in DRG is consistent with previous studies that used lumbar disc herniation models³⁵ but it contrasts with studies that used neuropathic pain models.^{36,37} These findings suggest that altered gene expression in sensory neurons are specific to the types of tissue injury. Interestingly, our findings showed a strong similarity to a transcriptomic analysis of the spinal cord in a similar model of post-operative pain by Raithel et al. by identifying increased inflammation as a possible contributing factor for pain development at day 2 after plantar incision.³⁸ Together, these two studies showed a prolonged common physiological response following plantar incision at the DRG and spinal cord. However, our findings showed an opposite effect from Raithel et al.³⁸ in cell proliferation. This differential effect could stem from differences in the timing (24 h vs. 48 h) or tissue type (DRG vs. spinal cord) of analysis

following plantar incision. Given a positive effects of the CEBPB and the PTGER2 in the genesis of neuropathic pain,³⁹ the reduced activity of these factors in the DRG of the incision model could have a role in wound repair. The role of the cell cycle regulator FOXM1 in post-operative pain is unknown. Due to its high expression level in macrophages, reduced FOXM1 activity could have a role in inflammatory response and wound repair following plantar incision.⁴⁰

Plantar incision induces Toll-like receptor 9 mediated pro-inflammatory response

Gene expression changes in the DRG suggest TLR9 as a significant regulator pain development following plantar incision (Figure 4(a) and (b)). Among the DRG genes, IFIT1b and ILR2a were profoundly upregulated

by 50- and 34-fold, respectively. TLRs signaling are thought to protect and defend the host organism by initiating inflammatory responses during tissue injury. Activation of TLRs in glia, sensory neurons, and other cell types has been shown to alter nociceptive processing leading to pain.⁴¹ Though our findings pinpoint TLR9 activation in the DRG as a contributing factor in a model of post-operative pain, this signaling mechanism has been postulated in neuropathic and inflammatory pain models.^{42,43} Thus, TLR9 activity is likely a common mechanism in DRG that modulates pain signaling in multiple pain models. Stimulation of TLR9 can exacerbate neuronal injury through excessive release of Tumor necrosis factor and nitric oxide from glial cells.⁴⁴ Conversely, inhibition of TLR9 signaling can reduce neuropathic pain⁴⁵ and thermal hyperalgesia following spinal cord injury.⁴⁶ TLR9 signals through MyD88, which activates the transcription factor NF- κ B for production of pro-inflammatory cytokines.⁴¹ Further studies are needed to determine the mechanisms by which TLR9 contributes to pain hypersensitivity following plantar incision.

Plantar incision inhibits IL10RA-mediated anti-inflammatory responses

The reduced DRG expression of *EDNRB*, *EMP2*, *FBN1* predicted the inhibition of upstream regulator interleukin 10 receptor (IL10RA) activity after plantar incision (Figure 4(c) and (d)). Emerging evidence indicates that IL-10 is a potent anti-inflammatory molecule that acts to dampen initial pro-inflammatory responses through a poorly defined feedback mechanism.⁴⁷ In addition, IL-10 is a positive regulator of neuropathic pain, where intrathecal administration of IL-10 attenuates mechanical allodynia and thermal hyperalgesia after chronic constriction injury of the sciatic nerves.⁴⁸ Moreover, IL-10 can be induced by electro-puncture to produce analgesic effects in the plantar incision model.⁴⁹ Our finding of reduced IL10RA activity suggests a role in modulating pain behaviors following plantar incision. More studies are needed to delineate the mechanism by which IL10 signaling contributes to the development of incisional pain.

Activation of IGF signaling pathway following plantar incision

We identified insulin-like growth factor signaling (IGF1, IGF-2, and IGF binding proteins) as a major gene network in the development of pain behaviors (Figure 5(a) to (c)). The upregulation of IGF2 and IGFBP6 after incision (Figure 5(d)) was ameliorated by capsaicin pretreatment, suggesting active roles of IGF2 and IGFBP6 in the development of incisional pain (Figure 7). IGF2 is

a neurotrophic factor critical for cell proliferation, neuronal survival, and nerve regeneration. Dysregulated IGF2 expression is implicated in a growing number of diseases.^{50–54} IGF2 binds with IGF1 receptor (IGF1R), IGF2R, and insulin receptors. Activation of IGF1-receptors engages multiple signaling pathways, including the PI3 kinase/AKT and MAPK, which modulate neuronal function and plasticity.^{55–58} Activation of IGF1R can stimulate voltage-gated T-type Ca²⁺ (CaV3) channels in mouse DRG through a mechanism dependent on heterotrimeric G protein signaling.^{59,60} The inhibition of IGF-1R signaling or knock down of CaV3 in DRG neurons abolished the increased mechanical and thermal sensitivity after chronic inflammation.⁶⁰ In addition, IGF-receptor activation enhanced TrpV1-mediated membrane currents in heterologous expression systems and cultured DRG neurons.⁶¹ We have previously shown that TrpV1 contributes to spontaneous activity and sensitization to heat of primary afferent nociceptors following skin incision in rats.²² Taken together, these findings suggest that IGF signaling is a novel pharmacologic target with therapeutic potential to manage pain following surgical procedures.

Conclusions

We highlight three signaling pathways in the DRG that are potentially involved in the processing of incisional pain. These pathways may modulate nociceptor activation and sensitization, tissue repair, nerve regeneration, and inflammatory responses. The present study is the first to employ NGS, which is a genome-wide approach to identify molecular factors, in the DRG of incisional pain model. Our data suggest that patterns of transcriptome changes after incision share similar processes in the development of pain associated with diabetes and inflammation^{12–16}; but distinct from neuropathic pain³⁷ and sciatic nerve transection³⁶ pain model, which include process for neuronal cell death and regeneration. This study is limited in its pathway predictions, which are based on a knowledge-based database, and a lack of validation at the protein level. While the transcriptomic changes that were attenuated by capsaicin pretreatment are likely associated with postoperative pain development, we cannot rule out the possibility of other non-pain-related processes contributed to these changes. Future studies are warranted to validate our results. Nevertheless, investigation of this process on a molecular level by examining whole-genome transcriptional activity provides initial insights into the mechanisms of incisional pain, which may ultimately guide efforts to identify novel therapeutics and biomarkers for incisional pain in the future.

Acknowledgments

The work is dedicated to Professor Timothy J Brennan, MD, PhD, Emeritus Professor of the Department of Anesthesiology, University of Iowa, on the eve of his retirement after many years of invaluable contribution to acute postoperative pain model and mechanism.

Declaration of Conflicting Interests

The author(s) declared no potential conflicts of interest with respect to the research, authorship, and/or publication of this article.

Funding

The author(s) disclosed receipt of the following financial support for the research, authorship, and/or publication of this article: This work was supported by a startup fund to RKB from the Department of Anesthesiology, University of Minnesota and Fairview Medical Center and in part by NIH grants HL135895 and CA241627 to DS.

ORCID iD

Ratan K Banik  <https://orcid.org/0000-0001-7126-5768>

References

- Weiser TG, Regenbogen SE, Thompson KD, Haynes AB, Lipsitz SR, Berry WR, Gawande AA. An estimation of the global volume of surgery: a modelling strategy based on available data. *Lancet* 2008; 372: 139–144.
- DeFrances CJ, Podgornik MN. National hospital discharge survey. *Adv Data* 2004; 2006: 1–19. <http://www.ncbi.nlm.nih.gov/pubmed/16703980>.
- Kehlet H, Jensen TS, Woolf CJ. Persistent postsurgical pain: risk factors and prevention. *Lancet (London, England)* 2006; 367: 1618–1625.
- Polomano RC, Dunwoody CJ, Krenzischek DA, Rathmell JP. Perspective on pain management in the 21st century. *Pain Manag Nurs* 2008; 9: 3–10.
- Imam MZ, Kuo A, Ghassabian S, Smith MT. Progress in understanding mechanisms of opioid-induced gastrointestinal adverse effects and respiratory depression. *Neuropharmacology* 2018; 131: 238–255.
- Dumas EO, Pollack GM. Opioid tolerance development: a pharmacokinetic/pharmacodynamic perspective. *Aaps J* 2008; 10: 537–551.
- Fletcher D, Martinez V. Opioid-induced hyperalgesia in patients after surgery: a systematic review and a meta-analysis. *Br J Anaesth* 2014; 112: 991–1004.
- de Boer HD, Detriche O, Forget P. Opioid-related side effects: postoperative ileus, urinary retention, nausea and vomiting, and shivering. A review of the literature. *Best Pract Res Clin Anaesthesiol* 2017; 31: 499–504.
- Boyer EW. Management of opioid analgesic overdose. *N Engl J Med* 2012; 367: 146–155.
- Alam A, Gomes T, Zheng H, Mamdani MM, Juurlink DN, Bell CM. Long-term analgesic use after low-risk surgery: a retrospective cohort study. *Arch Intern Med* 2012; 172: 425–430.
- Bates C, Laciak R, Southwick A, Bishoff J. Overprescription of postoperative narcotics: a look at postoperative pain medication delivery, consumption and disposal in urological practice. *J Urol* 2011; 185: 551–555.
- Athie MCP, Vieira AS, Teixeira JM, dos Santos GG, Dias EV, Tambeli CH, Sartori CR, Parada CA. Transcriptome analysis of dorsal root ganglia's diabetic neuropathy reveals mechanisms involved in pain and regeneration. *Life Sci* 2018; 205: 54–62.
- Pande M, Hur J, Hong Y, Backus C, Hayes JM, Oh SS, Kretzler M, Feldman EL. Transcriptional profiling of diabetic neuropathy in the BKS db/db mouse: a model of type 2 diabetes. *Diabetes* 2011; 60: 1981–1989.
- Perkins JR, Antunes-Martins A, Calvo M, Grist J, Rust W, Schmid R, Hildebrandt T, Kohl M, Orengo C, McMahon SB, Bennett DLH. A comparison of RNA-seq and exon arrays for whole genome transcription profiling of the L5 spinal nerve transection model of neuropathic pain in the rat. *Mol Pain* 2014; 10: 7.
- Wangzhou A, McIlvried LA, Paige C, Barragan-Iglesias P, Guzman CA, Dussor G, Ray PR, Gereau RW, Price TJ. Pharmacological target-focused transcriptomic analysis of native vs cultured human and mouse dorsal root ganglia. *Pain* 2020; 161(7): 1497–1517.
- Yin C, Hu Q, Liu B, Tai Y, Zheng X, Li Y, Xiang X, Wang P, Liu B. Transcriptome profiling of dorsal root ganglia in a rat model of complex regional pain syndrome type-I reveals potential mechanisms involved in pain. *J Pain Res* 2019; 12: 1201–1216.
- Haroutiunian S, Nikolajsen L, Finnerup NB, Jensen TS. The neuropathic component in persistent postsurgical pain: a systematic literature review. *Pain* 2013; 154: 95–102.
- Richebé P, Capdevila X, Rivat C. Persistent postsurgical pain: pathophysiology and preventative pharmacologic considerations. *Anesthesiology* 2018; 129: 590–607.
- Xu Q, Yaksh TL. A brief comparison of the pathophysiology of inflammatory versus neuropathic pain. *Curr Opin Anaesthesiol* 2011; 24: 400–407.
- Banik RK, Brennan TJ. Sensitization of primary afferents to mechanical and heat stimuli after incision in a novel in vitro mouse glabrous skin-nerve preparation. *Pain* 2008; 138: 380–391.
- Banik RK, Brennan TJ. Spontaneous discharge and increased heat sensitivity of rat C-fiber nociceptors are present in vitro after plantar incision. *Pain* 2004; 112: 204–213.
- Banik RK, Brennan TJ. Trpv1 mediates spontaneous firing and heat sensitization of cutaneous primary afferents after plantar incision. *Pain* 2009; 141: 41–51.
- Banik RK, Kabadi RA. A modified Hargreaves' method for assessing threshold temperatures for heat nociception. *J Neurosci Methods* 2013; 219: 41–51.
- Banik RK, Subieta AR, Wu C, Brennan TJ. Increased nerve growth factor after rat plantar incision contributes to guarding behavior and heat hyperalgesia. *Pain* 2005; 117: 68–76.

25. Kabadi R, Kouya F, Cohen HW, Banik RK. Spontaneous pain-like behaviors are more sensitive to morphine and buprenorphine than mechanically evoked behaviors in a rat model of acute postoperative pain. *Anesth Analg* 2015; 120: 472–478.
26. Kang S, Wu C, Banik RK, Brennan TJ. Effect of capsaicin treatment on nociceptors in rat glabrous skin one day after plantar incision. *Pain* 2010; 148: 128–140.
27. Uhelski ML, McAdams B, Johns ME, Kabadi RA, Simone DA, Banik RK. Lack of relationship between epidermal denervation by capsaicin and incisional pain behaviors: a laser scanning confocal microscopy study in rats. *Eur J Pain* 2020; 24: 1197–1208.
28. Kaliappan S, Simone DA, Banik RK. Nonlinear inverted-U shaped relationship between aging and epidermal innervation in the rat plantar hind paw: a laser scanning confocal microscopy study. *J Pain* 2018; 19: 1015–1023.
29. Kennedy WR, Wendelschafer-Crabb G, Johnson T. Quantitation of epidermal nerves in diabetic neuropathy. *Neurology* 1996; 47: 1042–1048.
30. Kim D, Langmead B, Salzberg SL. HISAT: a fast spliced aligner with low memory requirements. *Nat Methods* 2015; 12: 357–360.
31. McCarthy DJ, Chen Y, Smyth GK. Differential expression analysis of multifactor RNA-Seq experiments with respect to biological variation. *Nucleic Acids Res* 2012; 40: 4288–4297.
32. Robinson M, McCarthy D, Bioinformatics GS. edgeR: a Bioconductor package for differential expression analysis of digital gene expression data. *academic.oup.com n.d.*, <https://academic.oup.com/bioinformatics/article-abstract/26/1/139/182458> (2010, undefined.).
33. Tran PV, Kennedy BC, Pisansky MT, Won K-J, Gewirtz JC, Simmons RA, Georgieff MK. Prenatal choline supplementation diminishes early-life iron deficiency-induced reprogramming of molecular networks associated with behavioral abnormalities in the adult rat hippocampus. *J Nutr* 2016; 146: 484–493.
34. Spofford CM, Brennan TJ. Gene expression in skin, muscle, and dorsal root ganglion after plantar incision in the rat. *Anesthesiology* 2012; 117: 161–172.
35. Wang Q, Ai H, Liu J, Xu M, Zhou Z, Qian C, Xie Y, Yan J. Characterization of novel lnc RNAs in the spinal cord of rats with lumbar disc herniation. *J Pain Res* 2019; 12: 501–512.
36. Li S, Liu Q, Wang Y, Gu Y, Liu D, Wang C, Ding G, Chen J, Liu J, Gu X. Differential gene expression profiling and biological process analysis in proximal nerve segments after sciatic nerve transection. *PLoS One* 2013; 8: e57000.
37. Uttam S, Wong C, Amorim IS, Jafarnejad SM, Tansley SN, Yang J, Prager-Khoutorsky M, Mogil JS, Gkogkas CG, Khoutorsky A. Translational profiling of dorsal root ganglia and spinal cord in a mouse model of neuropathic pain. *Neurobiol Pain* 2018; 4: 35–44.
38. Raithel SJ, Sapio MR, LaPaglia DM, Iadarola MJ, Mannes AJ. Transcriptional changes in dorsal spinal cord persist after surgical incision despite preemptive analgesia with peripheral resiniferatoxin. *Anesthesiology* 2018; 128: 620–635.
39. Sasaki M, Hashimoto S, Sawa T, Amaya F. Tumor necrosis factor- α induces expression of C/EBP- β in primary afferent neurons following nerve injury. *Neuroscience* 2014; 279: 1–9.
40. Ren X, Zhang Y, Snyder J, Cross ER, Shah Ta Kalin TV, Kalinichenko VV. Forkhead box M1 transcription factor is required for macrophage recruitment during liver repair. *Mol Cell Biol* 2010; 30: 5381–5393.
41. Lacagnina MJ, Watkins LR, Grace PM. Toll-like receptors and their role in persistent pain. *Pharmacol Ther* 2018; 184: 145–158.
42. David BT, Ratnayake A, Amarante Ma Reddy Np Dong W, Sampath S, Heary RF, Elkabes SA. Toll-like receptor 9 antagonist reduces pain hypersensitivity and the inflammatory response in spinal cord injury. *Neurobiol Dis* 2013; 54: 194–205.
43. Luo X, Huh Y, Bang S, He Q, Zhang L, Matsuda M, Ji RR. Macrophage toll-like receptor 9 contributes to chemotherapy-induced neuropathic pain in male mice. *J Neurosci* 2019; 39: 6848–6864.
44. Iliev AI, Stringaris AK, Nau R, Neumann H. Neuronal injury mediated via stimulation of microglial toll-like receptor-9 (TLR9). *FASEB J* 2004; 18: 412–414.
45. Liu F, Wang Z, Qiu Y, Wei M, Li C, Xie Y, Shen L, Huang Y, Ma C. Suppression of MyD88-dependent signaling alleviates neuropathic pain induced by peripheral nerve injury in the rat. *J Neuroinflammation* 2017; 14: 70.
46. David BT, Ratnayake A, Amarante MA, Reddy NP, Dong W, Sampath S, Heary RF, Elkabes S. A toll-like receptor 9 antagonist reduces pain hypersensitivity and the inflammatory response in spinal cord injury. *Neurobiol Dis* 2013; 54: 194–205.
47. Iyer SS, Cheng G. Role of interleukin 10 transcriptional regulation in inflammation and autoimmune disease. *Crit Rev Immunol* 2012; 32: 23–63.
48. Milligan ED, Langer SJ, Sloane EM, He L, Wieseler-Frank J, O'Connor K, Martin D, Forsayeth JR, Maier SF, Johnson K, Chavez RA, Leinwand LA, Watkins LR. Controlling pathological pain by adenovirally driven spinal production of the anti-inflammatory cytokine, interleukin-10. *Eur J Neurosci* 2005; 21: 2136–2148.
49. Dai W, Sun J-L, Li C, Mao W, Huang Y-K, Zhao Z-Q, Zhang Y-Q, Lu N. Involvement of interleukin-10 in analgesia of electroacupuncture on incision pain. *Evidence-Based Complement Altern Med* 2019; 2019: 1–11.
50. Alvino CL, Ong SC, McNeil KA, Delaine C, Booker GW, Wallace JC, Forbes BE. Understanding the mechanism of insulin and insulin-like growth factor (IGF) receptor activation by IGF-II. *PLoS One* 2011; 6: e27488.
51. Bergman D, Halje M, Nordin M, Engström W. Insulin-like growth factor 2 in development and disease: a mini-review. *Gerontology* 2013; 59: 240–249.
52. Chao W, D'Amore P A. IGF2: epigenetic regulation and role in development and disease. *Cytokine Growth Factor Rev* 2008; 19: 111–120.
53. Clemmons DR. Insulin-like growth factor binding proteins and their role in controlling IGF actions. *Cytokine Growth Factor Rev* 1997; 8: 45–62.

54. Engström W, Shokrai A, Otte K, Granérus M, Gessbo Å, Bierke P, Madej A, Sjölund M, Ward A. Transcriptional regulation and biological significance of the insulin like growth factor II gene. *Cell Prolif* 1998; 31: 173–189.
55. Foncea R, Andersson M, Ketterman A, Blakesley V, Sapag-Hagar M, Sugden PH, LeRoith D, Lavandero S. Insulin-like growth factor-I rapidly activates multiple signal transduction pathways in cultured rat cardiac myocytes. *J Biol Chem* 1997; 272: 19115–19124.
56. Monnier D, Boutillier AL, Giraud P, Chiu R, Aunis D, Feltz P, Zwiller J, Loeffler JP. Insulin-like growth factor-I stimulates c-fos and c-jun transcription in PC12 cells. *Mol Cell Endocrinol* 1994; 104: 139–145.
57. Pugazhenti S, Boras T, O'Connor D, Meintzer MK, Heidenreich KA, Reusch JEB. Insulin-like growth factor I-mediated activation of the transcription factor camp response element-binding protein in pc12 cells: involvement of p38 mitogen-activated protein kinase-mediated pathway. *J Biol Chem* 1999; 274: 2829–2837.
58. Zheng WH, Quirion R. Insulin-like growth factor-1 (IGF-1) induces the activation/phosphorylation of Akt kinase and cAMP response element-binding protein (CREB) by activating different signaling pathways in PC12 cells. *BMC Neurosci* 2006; 7: 51.
59. Stemkowski PL, Zamponi GW. The tao of IGF-1: insulin-like growth factor receptor activation increases pain by enhancing T-type calcium channel activity. *Sci Signal* 2014; 7: pe23.
60. Zhang Y, Qin W, Qian Z, Liu X, Wang H, Gong S, Sun YG, Snutch TP, Jiang X, Tao J. Peripheral pain is enhanced by insulin-like growth factor 1 through a G protein-mediated stimulation of T-type calcium channels. *Sci Signal* 2014; 7: ra94.
61. Van Buren JJ, Bhat S, Rotello R, Pauza ME, Premkumar LS. Sensitization and translocation of TRPV1 by insulin and IGF-I. *Mol Pain* 2005; 1: 17.